Commun.Fac.Sci.Univ.Ank.Series B
Volume 61, Number 1-2, Pages 55-68(2019)
ISSN 2687-4806
http://communications.science.ankara.edu.tr/index.php?series=B

PROBING THE STRUCTURE-CORROSION INHIBITION PROPERTY RELATIONSHIP OF PYRROLE OLIGOMERS WITH DFT CALCULATIONS

GÖKHAN GECE, SEMRA BİLGİÇ

ABSTRACT. Density functional theory (DFT) calculations on pyrrole oligomers were carried out at the B3LYP/6-311+G(d,p) level to search the relationship between the molecular structure and corrosion inhibition. The electronic properties such as the highest occupied molecular orbital (HOMO), the lowest unoccupied molecular orbital (LUMO) energy levels, energy gap (LUMO-HOMO) and dipole moment were computed. It was found that these electronic values can explain some features of the inhibition phenomena.

1. INTRODUCTION

The annual cost of corrosion and of protection against corrosion in the world is staggering. A recent study estimates that the annual cost of corrosion in the U.S. alone is $276 billion [1]. Protection of oxidizable metals against corrosion is one application that has been intensively investigated [2]. Many corrosion control methods such as coating and conversion films have been proposed, but all such methods involve environmentally hazardous materials [3,4]. Therefore, there is a rigorous search underway for an environmentally friendly alternative to be used in corrosion control coatings [5,6]. One possible alternative are electroactive conducting polymers such as polypyrrole.

Following Deberry's work [7] on the corrosion-protective properties of polyaniline on stainless steel, several papers have been published describing corrosion studies of conducting polymers on various active metals [8-10]. It has been shown that polypyrrole coatings can prevent corrosion of oxidizable metals [11]. However, the protection mechanism is too complex and still under debate.

Recently, quantum chemical methods have become an effective way to study the corrosion inhibition [12] and much achievement was reached [13-15]. It is generally

Received by the editors: October 30, 2019; Accepted: December 03, 2019.
Key word and phrases: Pyrrole, Polypyrrole, Corrosion, Inhibition, Density Functional Theory

accepted that conducting polymers operate as corrosion inhibitors since they have multiple adsorption sites in their molecular structure [16], and there appears to be no reported work involving an adequate treatment of the quantum mechanics to understand of the role of pyrrole oligomers in corrosion inhibition.

On the basis of the above considerations, the aim of the present work was to investigate the underlying physical behavior for corrosion inhibition properties of small pyrrole oligomers up to heptapyrrole as models of the polypyrrole chain by using density functional theory (DFT) calculations.

2. Computational Methods

The calculations were performed by using the *Gaussian09* program [17] with the 6-311+G(d,p) basis set. The Becke three-parameter exchange-functional with non-local correction provided by the Lee-Yang-Parr (B3LYP) method was used. The molecular geometries were fully optimized. After geometry optimizations, harmonic vibrational frequencies have been calculated at the same level. Harmonic frequency analysis indicated that all stationary points were found to be true minima. It is very difficult to calculate parameters directly for an entire polymer molecule due to high molecular weights. However, oligomers can be used in such studies of polymers since all the properties depend on the chemical structure of the polymer molecule, and all this structure is conditioned by the oligomer structure. Therefore, in this study, oligomers composed from the central fragment (pyrrole) were accreted symmetrically and polypyrrole was modelled as a finite chain length of seven structural repeating units. The following quantum chemical indices were considered: the energy of the highest occupied molecular orbital (E_{HOMO}), the energy of the lowest unoccupied molecular orbital (E_{LUMO}), energy band gap, $\Delta E=E_{LUMO}-E_{HOMO}$ and dipole moment (μ).

3. Results And Discussion

The optimized molecular structure for pyrrole unit as a major and a repeat constituent of polypyrrole is depicted in Fig. 1. Experimental structural information on oligopyrroles is scarce, much theoretical discussion of π-conjugated systems such as polypyrrole begins with their representation as a linear, flat molecule. The important structural property of these structures is their planarity, which is directly related to the conjugation of π bond systems. Polypyrrole itself is planar in the solid [18] and gas-phase data are restricted to the microwave results of the pyrrole monomer [19]. In all cases, the geometry is found to be planar. This

geometry is consistent with the expectation of an uncharged π-conjugated system and with the results obtained for the oligomer versions of these polymers [20].

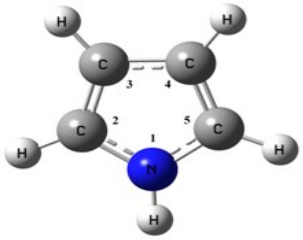

FIGURE 1. Optimized structure of pyrrole.

It is still controversial if polypyrrole exists only in the *anti* form or *syn* form at experimental conditions. The *anti* form has been found to be energetically more favorable [21], thus our theoretical calculations were conducted on planar *anti* structures of the pyrrole oligomers (Fig. 2). The geometrical parameters of the *anti* form of pyrrole are reported in Table 1 together with the experimental planar *anti* structure in the solid for comparison. In our case the structural parameters obtained by B3LYP/6-311+G(d,p) method are in the reasonable agreement with the relevant experimental results. It should be noted that in the case of the lowest molecular symmetries the results of calculations are closer to the experimental ones.

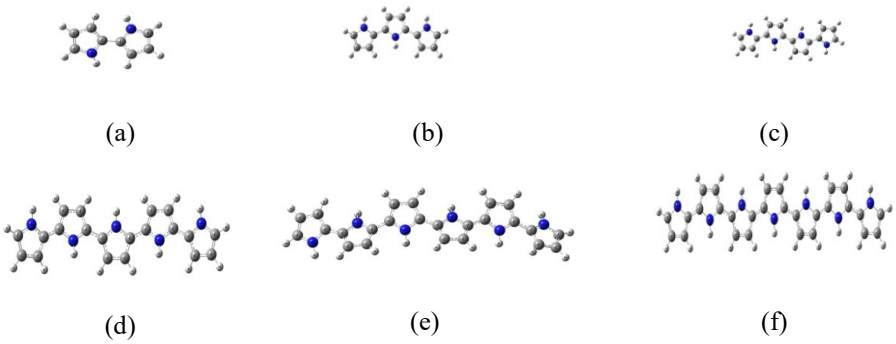

FIGURE 2. Optimized structures for (a) bipyrrole, (b) terpyrrole, (c) quarterpyrrole, (d) pentapyrrole, (e) hexapyrrole, (f) heptapyrrole.

TABLE 1. Optimized and experimental geometric parameters of pyrrole in the ground state.

	B3LYP/6-311+G(d,p)	Exp.[b]
Bond length (Å)[a]		
N1-C2	1.374	1.370
C2-C3	1.376	1.382
C3-C4	1.424	1.417
N1-H	1.006	0.996
C2-H	1.078	1.076
C3-H	1.077	1.077
Bond angle (º)[a]		
C2-N1-C5	109.8	109.8
N1-C2-C3	107.7	107.7
C2-C3-C4	107.4	107.4
H-C2-C3	131.1	130.8
H-C3-C2	125.7	125.5

[a] For numeration please see Fig. 1.
[b] Ref.[19].

According to the frontier molecular orbital theory, the formation of a transition state is due to an interaction between the frontier orbitals (HOMO and LUMO) of reactants [22]. The highest occupied molecular orbitals (HOMO) of the repeat units form the occupied π-band (valence band) of the polypyrrole and the lowest unoccupied molecular orbitals (LUMO) of the repeat unit form the π*-band (conduction band) of the polypyrrole. The energy distance between these two bands is defined as the band gap (ΔE), and in neutral conjugated polymers refers to the onset energy of the π-π* transition [23]. Accordingly, the energy of the highest occupied molecular orbital (E_{HOMO}), the energy of the lowest unoccupied molecular orbital (E_{LUMO}) and the energy gap ($\Delta E = E_{LUMO}$-E_{HOMO}) are important electronic properties that are related to the inhibition efficiency of polypyrrole. In the present work, these properties were examined. It is well known that the value of E_{HOMO} is often associated with the electron donating ability of the inhibitor molecule, higher values of E_{HOMO} indicate the greater ease of donating electrons to the unoccupied d orbital of the metal. The value of E_{LUMO} is related to the ability of the molecule to accept electrons, lower values of E_{LUMO} show the acceptance of

electrons by the inhibitor molecule. Consequently, the value of ΔE provides a measure for the stability of the formed complex [12].

E_{HOMO}, E_{LUMO} and ΔE data for the studied structures are summarized in Table 2. Table 3 shows the comparison of the values of ΔE for pyrrole, bipyrrole and polypyrrole with experimental data [24]. From these results it appears that the E_{HOMO} level increases and the E_{LUMO} level and the energy gap decrease with increasing chain length. This tendency also provides evidence that resulting from the molecular structure, the higher the HOMO energy of the polypyrrole, the greater the ease of offering electrons to unoccupied d orbitals of metal surface. The lower the LUMO energy, the easier the acceptance of electrons from the metal surface, which decreases HOMO-LUMO energy gap and improves the efficiency of the polypyrrole. The plots of E_{HOMO}, E_{LUMO} and ΔE as a function of the reciprocal of inverse chain length (CL=1/n) are given in Fig. 3. Plotting the calculated results against the inverse chain length is a commonly applied approach to discuss the polymer properties [25,26].

TABLE 2. Energetic data for the studied structures versus to the increasing chain length (CL).

Structure	E_{HOMO} (eV)	E_{LUMO} (eV)	$\Delta E(E_L-E_H)$ (eV)	CL (1/n)
Pyrrole	-5.946	-0.085	5.861	1
Bipyrrole	-5.098	-0.378	4.720	0.50
Terpyrrole	-4.782	-0.390	4.392	0.33
Quarterpyrrole	-4.676	-0.814	3.862	0.25
Pentapyrole	-4.573	-0.928	3.645	0.20
Hexapyrrole	-4.507	-1.004	3.503	0.16
Heptapyrrole	-4.432	-1.096	3.336	0.14

In order to calculate the effects of E_{HOMO}, E_{LUMO} and ΔE variables on the CL (1/n), a first-order design model was used according to the results given in Table 2. The general form of the first-order model in k independent variables $X_1,X_2,...,X_k$ is

$$Y = \beta_0 + \sum_{i=1}^{k} \beta_i X_i + \varepsilon \tag{3.1}$$

Where Y is an observable dependent variable, $\beta_o, \beta_1, \ldots, \beta_k$ are the unknown parameters and ε is a random error term [27]. In this study, CL $(1/n)$ is taken as a dependent variable and E_{HOMO}, E_{LUMO} and ΔE are considered as independent variables.

TABLE 3. Comparison of the ΔE values for pyrrole, bipyrrole and polypyrrole.

Structures	B3LYP/6-311+G(d,p)	Exp.[a]
Pyrrole	5.86	5.97
Bipyrrole	4.72	4.35
Polypyrrole	3.34	3.00

[a] Ref.[24].

The parameters of the model in equation (3.1) are estimated from the calculated results by applying the least squares method in Minitab 14 statistical software. Firstly, the effects of E_{HOMO}, E_{LUMO} and ΔE on the CL (1/n) are calculated individually. Then the relationship between all the independent variables and CL (1/n) is probed. The predicted models are given in the following equations:

$$CL = -2.44 - 0.577E_{HOMO} \quad (R^2 = 99.9\ \%) \tag{3.2}$$

$$CL = 0.841 + 0.705E_{LUMO} \quad (R^2 = 79.2\ \%) \tag{3.3}$$

$$CL = -1.04 + 0.336\,\Delta E \quad (R^2 = 95.9\ \%) \tag{3.4}$$

$$CL = -2.46 - 0.581E_{HOMO} - 0.0053E_{LUMO} \quad (R^2 = 99.9\ \%) \tag{3.5}$$

The obtained equations (3.3) and (3.4) show that E_{LUMO} and ΔE values increase with increasing values of CL $(1/n)$. Conversely, an increase in E_{HOMO} values causes a significant decrease in CL $(1/n)$ as in equation (3.2). In order to gain a better understanding of the results, the predicted models (3.2)-(3.4) are presented in Fig. 3. The slope of the line shows the negative correlation between the CL $(1/n)$ and E_{HOMO} variables in Fig. 3(a). It can be seen from the Fig. 3(b) and Fig. 3(c) that there is a positive correlation between the CL $(1/n)$ and independent variables.

When the effects of all independent variables are taken into consideration, the equation (3.5) gives a good predicted model. The ΔE has been neglected in this predicted model due to the

multicollinearity of ΔE with the E_{HOMO} and E_{LUMO}. Besides, the coefficient of E_{LUMO} is too small, -0.0053, to explain the variation on CL ($1/n$). It can be said that the coefficient of determination, R^2, is sufficient enough to explain the effect of E_{HOMO} on CL ($1/n$) for the models given in equations (3.2) and (3.5).

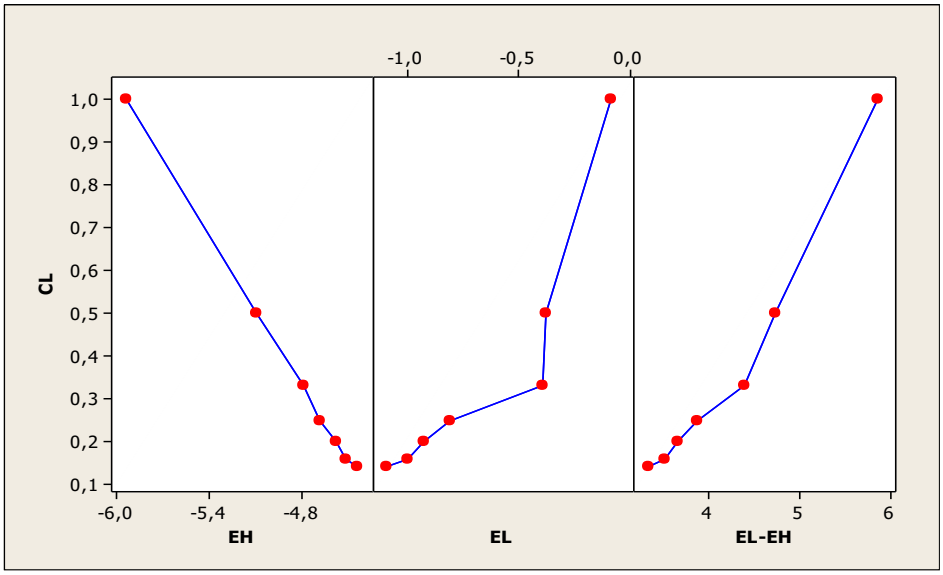

(a) b) (c)

FIGURE. 3. Predicted models of equations (3.2) - (3.4).

The observed and predicted values of CL ($1/n$) which are obtained using predicted model equations (3.2)-(3.5) are presented in Fig. 4. As can be seen, there is a good agreement between predicted values of equation (3.2), Pre2_CL, and observed data points, CL ($1/n$). Also, equation (3.5) gives good agreement with observed CL ($1/n$). The regression analysis shows that the E_{HOMO} is the most efficient variable on the CL ($1/n$).

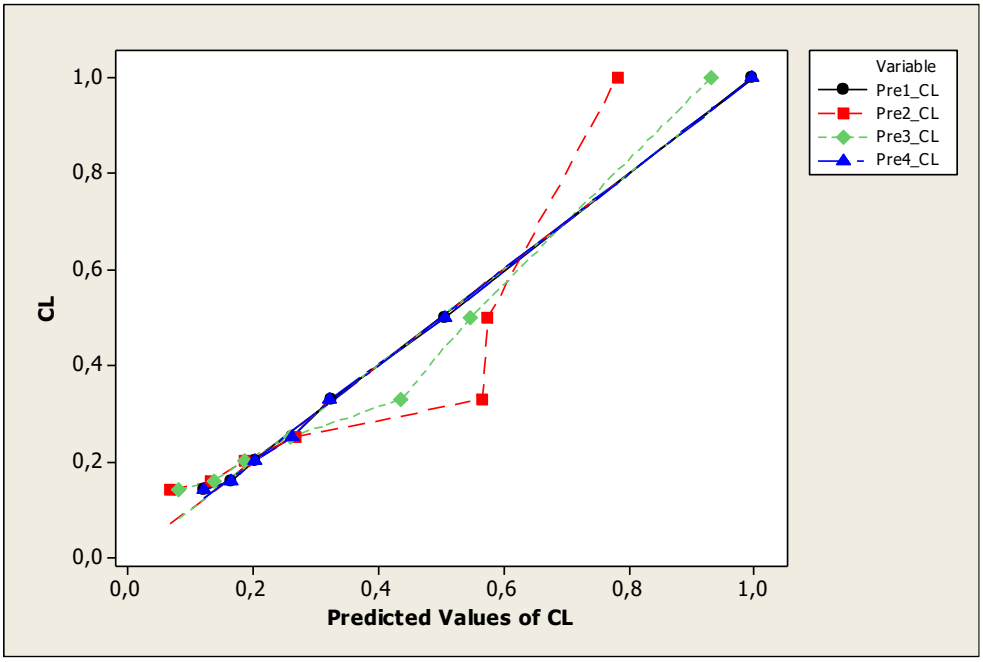

FIGURE 4. Relationship between experimental and predicted values of equations (3.2) - (3.5).

To determine the type of interaction between iron and the studied structures by a molecular approach, the energy differences of frontier orbitals of iron and pyrrole derivatives are considered in Table 4. The energies of HOMO and LUMO of iron were taken from the literature [28] equal to -7.81 and -0.25 eV, respectively. Since the gap of $E_{LUMO(Fe)}$ - $E_{HOMO(polypyrrole)}$ has much less value compared to, $E_{LUMO(polypyrrole)}$ - $E_{HOMO(Fe)}$, there is a strong possibility of electrons from polypyrrole to be given to iron, further strengthening the adsorption.

TABLE 4. HOMO-LUMO gap for the interaction of iron – polypyrrole.

	E_{HOMO} (eV)	E_{LUMO} (eV)	ΔE (eV)	
polypyrrole	-4.43	-1.09	6.72[a]	4.18[b]
iron	-7.81	-0.25		

[a] $E_{LUMO\ polypyrrole}$ - $E_{HOMO\ Fe}$

[b] $E_{LUMO\ Fe}$ - $E_{HOMO\ polypyrrole}$

The polarity of a molecule is well known to be important far various physicochemical properties and the most often used quantity to describe the polarity is the dipole moment (μ) of the molecule [29]. Pyrrole has a medium polarity with an experimental gas-phase dipole moment of 1.74 D [19]. In order to compare the polarization of pyrrole quantitatively with those of oligomers, the dipole moments (μ) were calculated by 6-311+G(d,p) DFT method. To validate the accuracy of the obtained values, the data from the literature [19,30,31] were also given in Table 5.

TABLE 5. Dipole moments (μ/Debye) of the studied structures.

	HF/6-31G(d)	MP2/6-31G(d)	B3LYP/6-31G(d)	B3LYP/6-311+G(d,p)	Exp.
Pyrrole	1.90[a]	1.98[a]/1.84[b]	1.91[a]	1.88	1.74[c]
Bipyrrole	1.80[a]		1.81[a]	0.85	
Terpyrrole				2.28	
Quarterpyrrole				1.59	
Pentapyrrole				2.32	
Hexapyrrole				2.61	
Polypyrrole				1.84	

[a] Ref. [30].
[b] Ref. [31].
[c] Ref. [19].

The dipole moment is essential in the transfer process of inhibitors to the metal surface and its effect on corrosion inhibition is an ambiguous issue. Some researchers assert the contributions of higher dipole moments to the physical adsorption of inhibitory acting molecules [32,33] while some affirm the effect of the lowest dipole moments [34,35]. As can be seen from Table 5, there is an irregularity in the values of dipole moment. Nevertheless, this irregular change proves the fact that the adsorption might not be arisen from the intermolecular electrostatic force.

There is also a dicrepancy in the literature for the calculated dipole moment (μ) values of pyrrole by ab initio methods. Millefiori and Alparone [30] reported the overestimation of dipole moment by a somewhat greater amount (14%) in MP2/6-31G* calculations, while Seio et al. [31] overestimated it by 5-6%. HF/6-31G* and B3LYP/6-31G* calculations also overestimate the dipole moment (μ) by 9-10%. It is evident that the theoretical data suffer from the lack of diffuse functions in the basis set and the difference is probably due to the use of basis set in which the exponents of the d-polarization functions were reduced to 0.25 to improve the accuracy of the dispersion attractions.

4. Conclusion

The calculations provide a theoretical explanation to some extent for the evaluation of corrosion inhibition efficiency of polypyrrole. It is found that the inhibiting action of pyrrole oligomers depends strongly on the electronic structure of the molecules and corrosion inhibition efficiency has certain relationships to the highest occupied molecular orbital (HOMO), the lowest unoccupied molecular orbital (LUMO) energy levels, and the energy gap (LUMO-HOMO).

Özet

Pirol oligomerlerinde yoğunluk fonksiyonel teorisi (DFT) hesaplamaları, moleküler yapı ve korozyon inhibisyonu arasındaki ilişkiyi araştırmak için B3LYP/6-311+G(d,p) seviyesinde yapılmıştır. En yüksek dolu moleküler orbital (HOMO), en düşük boş moleküler orbital (LUMO) enerji seviyeleri, enerji boşluğu (LUMO-HOMO) ve dipol moment gibi elektronik özellikler hesaplanmıştır. Bu elektronik değerlerin inhibisyon olayının bazı özelliklerini açıklayabildiği bulunmuştur.

References

[1] G. H. Koch, M. P. H. Brongers, N. G. Thompson, Y. P. Virmani and J. H. Payer, Corrosion costs and preventive strategies in the United States. U.S. Federal Highway Administration Report, 2002.

[2] F. Presuel-Moreno, M. A. Jakab, N. Tailleart, M. Goldman and J. R. Scully, Corrosion-resistant metallic coatings. Materials Today 11 (2008) 14-23.

[3] G. O. Ilevbare, J. Yuan, R. G. Kelly and J. R. Scully, Inhibition of the corrosion of AA 2024: chromate conversion coating versus chromate additions. Corrosion 56 (2000) 227-242.

[4] I. M. Zin, R. L. Howard, S. J. Badger, J. D. Scantlebury and S. B. Lyon, The mode of action of chromate inhibitor in epoxy primer on galvanized steel. Progress in Organic Coatings 33 (1998) 203-210.

[5] M. Bazzaoui, J. I. Martins, E. A. Bazzaoui, T. C. Reis and L. Martins, Pyrrole electropolymerization on copper and brass in a single-step process from aqueous solution. Journal of Applied Electrochemistry 34 (2004) 815-822.

[6] B. N. Grgur, N. V. Krstajić, M. V. Vojnović, Č. Lačnjevac and Lj. Gajić-Krstajić, The influence of polypyrrole films on the corrosion behavior of iron in acid sulfate solutions. Progress in Organic Coatings 33 (1998) 1-6.

[7] D. W. Deberry, Modification of the electrochemical and corrosion behavior of stainless steels with an electroactive coating. Journal of the Electrochemical Society 132 (19859 1022-1026.

[8] A. Michalik and M. Rohwerder, Conducting polymers for corrosion protection: a critical view. Zeitschrift für Physikalische Chemie, 219 (2005) 1547-1559.

[9] P. Zarras, N. Anderson, C. Webber, D. J. Irwin, A. Guenthner and J.D. Stenger-Smith, Progress in using conductive polymers as corrosion-inhibiting coatings. Radiation Physics and Chemistry 68 (2003) 387-394.

[10] H. Nguyen Thi Le, M. C. Bernard, B. Garcia-Renaud and C. Deslouis, Raman spectroscopy analysis of polypyrrole films as protective coatings on iron. Synthetic Metals, 140 (2004) 287-293.

[11] J. Reut, A. Öpik and K. Idla, Corrosion behavior of polypyrrole coated mild steel. Synthetic Metals, 102 (1999) 1392-1393.

[12] G. Gece, The use of quantum chemical methods in corrosion inhibitor studies. Corrosion Science, 50 (2008) 2981-2992.

[13] L. T. Jr. Sein, Y. Wei and S. A. Jansen, The role of adsorption of aniline trimers on the corrosion inhibition process : a ZINDO/1 study. Computational and Theoretical Polymer Science, 11 (2001) 83-88.

[14] L. T. Jr. Sein, Y. Wei and S. A. Jansen, Corrosion inhibition by aniline oligomers through charge transfer: a DFT approach. Synthetic Metals 143 (2004) 1-12.

[15] A. Yurt, V. Bütün and B. Duran, Effect of the molecular weight and structure of some novel water-soluble triblock copolymers on the electrochemical behaviour of mild steel. Materials Chemistry and Physics 105 (2007) 114-121.

[16] R. Hasanov, S. Bilgiç and G. Gece, Experimental and theoretical studies on the corrosion properties of some conducting polymer coatings. Journal of Solid State Electrochemistry 15 (2011) 1063-1070.

[17] M. J. Frisch, G. W. Trucks, H. B. Schlegel, G. E. Scuseria, M. A. Robb, J. R. Cheeseman, G. Scalmani, V. Barone, G. A. Petersson, H. Nakatsuji, X. Li, M. Caricato, A. Marenich, J. Bloino, B. G. Janesko, R. Gomperts, B. Mennucci, H. P. Hratchian, J. V. Ortiz, A. F. Izmaylov, J. L. Sonnenberg, D. Williams-Young, F. Ding, F. Lipparini, F. Egidi, J. Goings, B. Peng, A. Petrone, T. Henderson, D. Ranasinghe, V. G. Zakrzewski, J. Gao, N. Rega, G. Zheng, W. Liang, M. Hada, M. Ehara, K. Toyota, R. Fukuda, J. Hasegawa, M. Ishida, T. Nakajima, Y. Honda, O. Kitao, H. Nakai, T. Vreven, K. Throssell, J. A. Montgomery, Jr., J. E. Peralta, F. Ogliaro, M. Bearpark, J. J. Heyd, E. Brothers, K. N. Kudin, V. N. Staroverov, T. Keith, R. Kobayashi, J. Normand, K. Raghavachari, A. Rendell, J. C. Burant, S. S. Iyengar, J. Tomasi, M. Cossi, J. M. Millam, M. Klene, C. Adamo, R. Cammi, J. W. Ochterski, R. L. Martin, K. Morokuma, O. Farkas, J. B. Foresman and D. J. Fox, Gaussian 09, Revision B.01, Gaussian, Inc., Wallingford CT, 2009.

[18] T. A. Skotheim, R. L. Elsenbaumer and J. R. Reynolds, Handbook of conducting polymers, Marcel Dekker Inc. New York, 1998.

[19] L. Nygaard, J.T. Nielsen, J. Kirchheiner, G. Maltesen, J. Rastrup-Andersen and G.O. Sørensen, Microwave spectra of isotopic pyrroles. Molecular structure, dipole moment, and ^{14}N quadrupole coupling constants of pyrrole. Journal of Molecular Structure, 3 (1969) 491-506.

[20] G. R. Hutchison, M. A. Ratner and T. J. Marks, Accurate prediction of band gaps in neutral heterocyclic conjugated polymers. Journal of Physical Chemistry A, 106 (2002) 10596-10605.

[21] T. Tamm, J. Tamm and M. Karelson, Theoretical study of the effect of counterions on the structure of pyrrole oligomers. International Journal of Quantum Chemistry, 88 (2002) 296-301.

[22] K. Fukui, Theory of orientation and stereoselection, Springer-Verlag, New York, 1975.

[23] J. Casanovas, E. Armelin, J. I. Iribarren, C. Alemán and F. Liesa, La modelización molecular como herramienta para el diseño de nuevos polímeros conductores. Polimeros, 15 (20059 239-244.

[24] J. L. Brédas, R. Silbey, D. S. Boudreaux and R. R. Chance, Chain-length dependence of electronic and electrochemical properties of conjugated systems - polyacetylene, polyphenylene, polythiophene, and polypyrrole. Journal of the American Chemical Society, 105 (1983) 6555-6559.

[25] G. Zotti, S. Martina, G. Wegner and A. D. Schlüter, Well-defined pyrrole oligomers: electrochemical and UV/vis studies. Advanced Materials, 4 (1992) 798-801.

[26] P. Audebert, J. M. Catel, G. L. Coustumer, V. Duchenet and P. Hapiot, Electrochemical oxidation of five-unit heterocycles: a discussion on the possible dimerization mechanisms. Journal of Physical Chemistry, 99 (1995) 11923-11929.

[27] A. I. Khuri and J. A. Cornell, Response surfaces: Designs and analyses, 2nd ed., (Marcel Dekker Inc., New York, 1996).

[28] P. Mutombo and N. Hackerman, The effect of some organophosphorus compounds on the corrosion behaviour of iron 6 M HCl. Anti-Corrosion Methods and Materials, 45 (1998) 413-418.

[29] M. Karelson and V. S. Lobanov, Quantum chemical descriptors in QSAR/QSPR studies. Chemical Reviews, 96 (1996) 1027-1043.

[30] S. Millefiori and A. Alparone, Ab initio and density functional theory study of the structure and torsional potential of pyrrole oligomers. Journal of Chemical Society Faraday Transactions, 94 (1998) 25-32.

[31] K. Seio, H. Ukawa, K. Shohda and M. Sekine, Computational evaluation of intermolecular interactions of a universal base 3-nitropyrrole in stacked dimers and DNA duplexes. Journal of Biomolecular Structure and Dynamics, 22 (2005) 735-746.

[32] A. Stoyanova, G. Petkova and S. D. Peyerimhoff, Correlation between the molecular structure and the corrosion inhibiting effect of some pyrophthalone compounds. Chemical Physics, 279 (2002) 1-6.

[33] X. Pang, B. Hou, W. Li, F. Liu, and Z. Yu, 2,3,5-triphenyl-2h-tetrazolium chloride and 2,4,6-tri(2-pyridyl)-s-triazine on the corrosion of mild steel in HCI. Chinese Journal of Chemical Engineering, 15 (2007) 909-915.

[34] M. Finšgar, A. Lesar, A. Kokalj and I. Milošev, A comparative electrochemical and quantum chemical calculation study of BTAH and BTAOH as copper corrosion inhibitors in near neutral chloride solution. Electrochimica Acta, 53 (2008) 8287-8297.

[35] Y. Yan, W. Li, L. Cai and B. Hou, Electrochemical and quantum chemical study of purines as corrosion inhibitors for mild steel in 1 M HCl solution. Electrochimica Acta, 53 (2008) 5953-5960.

Current Address: GÖKHAN GECE (Corresponding author): Department of Chemistry, Bursa Technical University, 16310 Bursa, Turkey.
E-mail Address: gokhangc@gmail.com
ORCID: https://orcid.org/0000-0001-9310-5407

Current Address: SEMRA BİLGİÇ: Department of Chemistry, Ankara University, 06100 Ankara, Turkey.
E-mail Address: bilgic@science.ankara.edu.tr
ORCID: https://orcid.org/0000-0001-9730-0146